The Journal of Experimental Biology 212, 3156-3163
Published by The Company of Biologists 2009
doi:10.1242/jeb.029249

Oxygen tension correlates with regional blood flow in obstructed rat kidney

Anja M. Jensen[1,2,3,*], Rikke Nørregaard[1,2], Sukru Oguzkan Topcu[1,2], Jørgen Frøkiær[1,2,3] and Michael Pedersen[2,4]

[1]The Water and Salt Research Center, [2]Institute of Clinical Medicine, [3]Department of Clinical Physiology and Nuclear Medicine and [4]MR Research Center, Aarhus University Hospital, Skejby, DK 8200, Aarhus N, Denmark

*Author for correspondence (anja.jensen@ki.au.dk)

Accepted 29 June 2009

SUMMARY

As renal tissue oxygen tension (P_{O_2}) is determined by the balance between oxygen supply and consumption, direct tissue P_{O_2} measurements are essential when evaluating the presence of hypoxia. The present study aimed at evaluating invasively and continuously the renal medullary and cortical tissue P_{O_2} by novel fibre-optic probes in rats subjected to acute unilateral ureteral obstruction (AUUO). In parallel, regional blood flow measurements were obtained by MRI to investigate the relationship between regional blood flow and tissue oxygen tension. The abundance of transport proteins was determined by immunoblotting. In the obstructed kidney, AUUO caused a prompt decrease in medullary tissue P_{O_2} to 60% of baseline level whereas cortical tissue P_{O_2} was unchanged. By contrast, tissue P_{O_2} slightly increased in the non-obstructed kidney. These changes developed during the first 30 min after AUUO and persisted for the 3 h observation period. Medullary blood flow declined 1.5–2 h after induction of AUUO to 61% of baseline level in the obstructed kidney. By contrast, cortical blood flow increased to 108% of baseline level in the non-obstructed kidney. Finally, the abundance of phosphorylated aquaporin 2 decreased significantly in the obstructed kidney medulla, but increased in the obstructed kidney cortex. The Na^+/K^+-ATPase abundance increased in the obstructed kidney medulla whereas the $Na^+/K^+/2Cl^-$ co-transporter abundance remained unchanged in the obstructed kidney. In conclusion, measurements of regional blood flow reflect tissue P_{O_2} changes during AUUO suggesting that reduced regional blood flow is a predictor of local hypoxia. Furthermore, the abundance of major transport protein is independent of tissue P_{O_2}.

Key words: kidney, hypoxia, perfusion.

INTRODUCTION

Local oxygen tension reflects the balance between oxygen delivery and oxygen consumption (Brezis et al., 1994a; Brezis et al., 1994b), making direct tissue oxygen measurements essential when evaluating the presence of potential regional hypoxia. The kidney is particularly vulnerable to medullary ischemia as the renal medulla of mammalian kidneys operates in a state of relative hypoxia (Neuhofer and Beck, 2006) predominantly as a result of relatively small inner-medullary blood flow (Brezis and Rosen, 1995). In parallel, as the delivery of oxygen to the medulla depends on cortical oxygen tension, the occurrence of cortical hypoxia may reduce medullary oxygen tension (O'Connor et al., 2006). The primary oxygen consuming activity in the kidney is tubular reabsorption of electrolytes, facilitated specifically by sodium transport proteins. The oxygen-consuming Na^+/K^+-ATPase localized along the entire nephron drives the secondary active sodium transport mediated by various sodium transport proteins, amongst others, the $Na^+/K^+/2Cl^-$ co-transporter (NKCC2) in the medullary thick ascending limb (TAL) of Henle's loop. Previous studies have revealed a reduced abundance and activity of these sodium transport proteins in response to ischemia (Kiroytcheva et al., 1999; Van Why et al., 1994; Wang et al., 1998). Furthermore, medullary oxygen tension increases in rats treated with furosemide which blocks NKCC2 (Brezis et al., 1994a). Besides electrolyte reabsorption, urine concentration requires high collecting duct water permeability, allowing the osmotically driven movement of water from the lumen to the interstitium. This is accomplished by aquaporin (AQP2) phosphorylation followed by insertion of AQP2-bearing subapical vesicles into the apical membrane of the collecting duct principal cells (Nielsen et al., 2002).

The renal blood distribution is complex and differently regulated in specific regions. Therefore, the kidney constitutes an ideal organ to study whether regional blood flow reflects local tissue oxygen tension. Furthermore, acute unilateral ureteral obstruction (AUUO) results in marked haemodynamic changes in the ipsilateral, obstructed kidney, usually characterized by an early hyperaemic phase (1–2 h), increasing renal blood flow (RBF) (Dal et al., 1977), and then by a vasoconstrictive phase (>3 h), showing reduced RBF (Harris and Yarger, 1974; Moody et al., 1975). The regional blood flow distribution during AUUO has been intensively investigated and the dominant finding is a reduced medullary blood flow (MBF) as early as 30 min after onset of the obstruction (Schwartz et al., 1977; Solez et al., 1976; Sweeney et al., 2001; Wahlberg et al., 1984). The cortical blood flow (CBF) has usually been found to have a pattern similar to the total RBF (Sweeney et al., 2001; Wahlberg et al., 1984), except in a study by Chen et al., who demonstrated that AUUO immediately reduces CBF in the obstructed rat kidney (Chen et al., 2001). Blood flow in the contralateral, non-obstructed kidney is less well described, but the few studies done indicate that it either remains stable or increases slightly (Heyman et al., 1997; Solez et al., 1976; Wahlberg et al., 1984). Accordingly, AUUO is suspected to cause medullary hypoxia in the obstructed kidney because of a reduced MBF and oxygen uptake. However, this correlation has, to our knowledge, never been demonstrated experimentally and thus AUUO constitutes a useful model for studying whether regional blood flow measurements are useful for estimation of tissue oxygen tension in specific organ regions.

We hypothesize that AUUO provokes prompt changes in the intrarenal blood supply in parallel with counter current regulations in local oxygen tension. Thus, the present study aimed to evaluate

invasively and continuously the local oxygen tension in the renal tissue using novel fibre-optic probes, and was performed simultaneously in both cortical and medullary parts of the kidney in an AUUO rat model. The regional renal blood flow during AUUO was evaluated non-invasively by magnetic resonance imaging (MRI). Finally, the abundance of major sodium transport proteins and aquaporins was determined in specific kidney zones to evaluate whether local oxygen tension regulates the abundance of transport proteins involved in the oxygen-consuming tubular transport mechanisms.

MATERIALS AND METHODS

Ethical approval

The animal protocols were approved by the board at the Institute of Clinical Medicine, University of Aarhus, according to the licenses for use of experimental animal issued by the Danish Ministry of Justice.

Animal handling

The study was performed with male Munich-Wistar rats (*Ratus norvegicus albinus* Berkenhaut 1769) weighing 250 g (Møllegaard, Aarhus, Denmark).

Protocol 1

Unilateral ureteral obstruction (UUO) was induced and simultaneous measurements of partial pressure of oxygen (P_{O_2}) of obstructed and non-obstructed cortex and medulla were measured in each animal with oxygen-sensitive sensors secured in a fixed position throughout the entire experimental protocol (0–3 h, N=8). Sham-operated controls were prepared in parallel (N=3). A period of 5 min was used to normalize the mean P_{O_2} level to 100%. In the UUO group, obstruction was initiated after 10 min, and P_{O_2} was successively recorded for up to 3 h at 15 s intervals.

Protocol 2

UUO was induced (N=5) and sham-operated controls were prepared in parallel (N=7). CBF and MBF were determined by MRI before and at 1.5–2 h after onset of the obstruction.

Protocol 3

UUO was induced for 2 h (N=7) and sham-operated controls were prepared in parallel (N=7). The kidneys were removed and prepared for immunoblotting.

Surgical procedure

The rats were inhalation anaesthetized with 2% isoflurane (Abbott, Solna, Sweden) in conjunction with O_2 (2 l min^{-1}) and nitrous oxide (0.2 l min^{-1}) and placed on a heating pad to maintain rectal temperature at 37–38°C during the entire experimental period in all three protocols. The left ureter was exposed through a midline abdominal incision, and the midportion of the ureter was occluded with a 3-0 silk ligature. Sham-operated controls were prepared in parallel. Protocol 1: before obstruction, the oxygen optodes were placed and secured in a fixed position in the two kidney zones (cortex and medulla), and the kidney surface was covered with a cotton swap wetted with saline. Baseline P_{O_2} was measured for 10 min before ureteral obstruction was induced.

Optical measurement of molecular oxygen (protocol 1)

For optical measurement of partial pressure of molecular oxygen, a novel micro-optode sensor was used (PreSense GmbH, Regensburg, Germany), consisting of a laser light source to illuminate the sensor, an optical fibre as signal transducer, a photo detector and the optical sensor. The micro-optode consists of a plastic syringe (diameter=7 mm), which houses the optical fibre with the optical sensor on its tapered tip (diameter=30 μm). The mechanism behind this fibre micro-optode is described by Gansert et al. (Gansert et al., 2001). In brief, oxygen as a triplet molecule is able to quench the fluorescence and phosphorescence of certain luminophores. This effect is called dynamic fluorescence quenching. The relationship between the oxygen concentration in the sample and the luminescence intensity, as well as the luminescence lifetime, is described by the Stern–Volmer equation:

$$\frac{I}{I_0} = \frac{\tau}{\tau_0} = \frac{1}{1 + K\left[\mathrm{O_2}\right]}, \quad (1)$$

where I_0 and I are the luminescence intensities in the absence and presence of oxygen, and τ_0 and τ are the respective luminescence lifetimes. The quenching constant K quantifies the quenching efficiency and therefore the sensitivity of the sensor. The quenching effect is highly specific for molecular oxygen. Effects of varying pH, ionic species and other solutes in the sample are avoided by embedding the oxygen sensitive indicator (the luminophore) in an ion-impermeable matrix. In contrast to amperometric oxygen electrodes, micro-optodes are in a thermodynamic equilibrium and not in a steady state. Therefore, no oxygen is consumed during the measurement and the signal is independent of changes in flow velocity. The system measures the luminescence lifetime of the immobilized luminophore as the oxygen-dependent parameter. The luminophore is applied as an extremely thin coating on the tip of the optical fibre. A phase-modulation technique is used to evaluate the lifetime of the indicators. If the luminophore is excited with a frequency-modulated light source, its lifetime causes a time delay of the emitted light signal. In other words, this delay is the phase angle between the exciting and the emitted signal. The phase angle is shifted as a function of the oxygen concentration and is inversely proportional to it. For calibration, the micro-optode-specific phase angle in air-saturated water (Φ_{20}) and in oxygen-free water (Φ_0) need to be determined over the operational temperature range of the experiment. The quenching constant (K) is calculated as:

$$K = \frac{1}{\mathrm{TAN}(\Phi_{20}) / \mathrm{TAN}(\Phi_0) - 1 + f} \Big/ 100\%, \quad (2)$$

where f is a constant value for a given sensor type. We used a sensor type with 37.5 kHz excitation frequency (f=0.85). Since Φ_{20} and Φ_0 change nearly linearly with temperature, K is also a nearly linear function of temperature within the range 2–30°C. The oxygen concentration (C_{O_2}) in water as a percentage of air saturation at a given temperature is then calculated as:

$$\mathrm{C_{O_2}} = \frac{\mathrm{TAN}(\Phi_m) / \mathrm{TAN}(\Phi_0)}{K\left[\mathrm{TAN}(\Phi_m) / \mathrm{TAN}(\Phi_0)\right] - 1 + f}, \quad (3)$$

with Φ_m the measured value of the phase angle. According to Henry's law, the saturated C_{O_2} in water is most simply calculated as:

$$\mathrm{C_{O_2}} = \frac{P_{O_2} C_w}{K_{O_2}}, \quad (4)$$

where P_{O_2} is the partial pressure of oxygen in air at atmospheric conditions, C_W the number of moles H_2O per litre and K_{O_2} the solubility coefficient of oxygen in water. The temperature dependence of K_{O_2} can be calculated as:

$$K_{O2} = 0.0729 \times T + 2.694, \quad (5)$$

derived from linear regression analysis of K_{O_2} values determined at different temperatures (Von Willert et al., 1995).

Measurements of renal blood flow (protocol 2)

Magnetic resonance imaging was performed with a Philips Intera 1.5 T clinical system (Philips Medical Systems, Best, The Netherlands) equipped with actively shielded magnetic field gradients with a maximal amplitude of 23 mT m^{-1}. Radiofrequency excitation was performed using the integrated body-coil. For radiofrequency reception, a surface coil with a diameter of 4 cm was employed. The animal was placed supine with the kidneys placed above the imaging coil.

To avoid movements of the kidneys during free breathing and magnetic susceptibility artefacts related to the adjoining bowel, an in-house-made plastic holder was used to block the movements of the kidneys and isolate them from bowel loops while avoiding compression of the parenchyma and renal vessels. High-resolution T2-weighted images were initially generated by a spin-echo pulse sequence to allow accurate discrimination between cortical and medullary components. Sequence parameters were as follows: recovery time (t_R)=2500 ms, echo time (t_E)=100 ms, slice thickness=2 mm, field-of-view=13×10 cm, and the acquisition and reconstruction matrix was 256×256. Number of data averages was 16 to improve the signal-to-noise ratio.

Perfusion weighted imaging was employed using a dynamic susceptibility weighted fast gradient echo sequence. Approximately 10 s after start of data acquisition, a single bolus of the iron-containing agent Sinarem (Guerbet, Paris, France) was administered rapidly in less than one second, which corresponded to a dose of 90 μmol Fe kg^{-1}. A dynamic series of 120 images was obtained using the following sequence parameters: t_R/t_E/flip angle= 12 ms/4 ms/9 deg., allowing images to be acquired with an interval of 0.6 s. Acquired slice thickness was 2 mm, and acquired spatial resolution was 64×128, but reconstructed to a 256×256 matrix to allow overlaying upon the anatomical weighted image. Analyses were done according to Aumann et al. (Aumann et al., 2003), using the software Mistar (Apollo Imaging Techology, Melbourne, Australia) with a two compartment model incorporating a deconvolution of an arterial input function with the renal tissue response.

Membrane fractionation for immunoblotting (protocol 3)

The tissue [in the three zones: cortex, inner stripe of outer medulla (ISOM), and inner medulla (IM)] were homogenized by an Ultra-Turrax T8 homogenizer (IKA Labortechnik, Staufen, Germany) in ice-cold isolation solution containing 0.3 mol l^{-1} sucrose, 25 mmol l^{-1} imidazole, 1 mmol l^{-1} EDTA, 8.5 μmol l^{-1} leupeptin (Sigma-Aldrich, St Louis, MO, USA), 0.4 mmol l^{-1} pefabloc (Roche, Basel, Switzerland), and for IM: sodium orthovanadate (Sigma-Aldrich), NaF (Merck, Whitehouse Station, NJ, USA), and okadic acid (Calbiochem, San Diego, CA, USA), pH 7.2. The homogenates were centrifuged at 1000 ***g*** for 15 min at 4°C to remove whole cells, nuclei and mitochondria. Gel samples were prepared from the supernatant in Laemmli sample buffer containing 2% SDS and dithiothreitol. The total protein concentration of the homogenate was measured using a Pierce BCA protein assay kit (Roche, Basel, Switzerland).

Electrophoresis and immunoblotting (protocol 3)

Membrane fractionation samples were run on 12% polyacrylamide gels (Bio-Rad, Mini Protean II, Hercules, CA, USA). For each gel, an identical gel was run in parallel and subjected to Coomassie Blue staining. The Coomassie-Blue-stained gel was run to ascertain identical loading or to allow for correction. The proteins were transferred to a nitrocellulose membrane (Hybond ECL RPN3032D, Amersham Pharmacia Biotech now GE Healthcare, Uppsala, Sweden) and after transfer, the blots were blocked with 5% milk in PBS-T (80 mmol l^{-1} Na_2HPO_4, 20 mmol l^{-1} NaH_2PO_4, 100 mmol l^{-1} NaCl, 0.1% Tween 20, pH 7.5), and incubated overnight at 4°C with primary antibodies. The antigen–antibody complex was visualized with horseradish peroxidase-conjugated secondary antibodies (P448 or P447, 1:3000; DAKO, Glostrup, Denmark) using the enhanced chemiluminescence system (Amersham Pharmacia Biotech). The ECL films were scanned using a Hewlett-Packed Scanjet scanner and densitometry was performed on the bands using the NIH ImageJ densitometric analysis software.

Primary antibodies (protocol 3)

For semi-quantitative immunoblotting we used previously characterized antibodies as follows: (1) an affinity-purified polyclonal antibody to AQP2 (Nielsen et al., 2006), (2) a monoclonal antibody against the α_1-subunit of Na^+/K^+-ATPase (Kashgarian et al., 1985), (3) an affinity-purified polyclonal antibody to AQP2 phosphorylated at serine 256 (KO407), a new antibody raised against the same sequence of immunizing peptide (GRRQS(*P*)VELHSPC) as previously described (Christensen et al., 2000), (4) an affinity-purified polyclonal antibody to NKCC2 (1495), a new antibody raised against the same sequence of immunizing peptide (EYYRNTGSVSGPKVNRPSLQEC) as previously described (Ecelbarger et al., 1996). The specificity of these two new antibodies was evaluated by, (1) detection of the immunizing peptide on dot-blots using immune serum, (2) detection of pS256-AQP2 and NKCC2 in a rat kidney protein sample on immunoblots using affinity-purified antibody showing bands identical to those seen with the previously characterized antibodies, and (3) ablation of pS256-AQP2 and NKCC2 detection when antibodies are pre-incubated with the immunizing peptide.

Statistical analysis

Measurements of P_{O_2} relative to baseline levels were averaged for all animals, and the plots (mean ± s.d.) of cortex and medullar were made for both the obstructed and non-obstructed kidney. MBF and CBF measurements relative to baseline levels were averaged for all animals (mean ± s.e.m.). Statistical comparisons (control kidney *versus* obstructed kidney and control kidney *versus* non-obstructed kidney) were calculated using unpaired *t*-tests for normally distributed data, or by a Mann–Whitney rank-sum test (immunoblotting of Na^+/K^+-ATPase in cortex). The densitometric data derived from the immunoblotting is presented as a percentage of the sham-operated levels. Statistical analysis was performed on percentage data and is presented as mean ± s.e.m. *P*-values of <0.05 were considered statistically significant.

RESULTS

Unilateral ureteral obstruction promptly reduces renal medullary tissue oxygen tension

Consecutive P_{O_2} measurements following AUUO revealed a rapid decrease in renal medullary tissue oxygen tension in the obstructed kidney during the first 30 min after onset of the obstruction to 60% of baseline levels, which persisted during the remaining observation period (in total 3 h; Fig. 1B). Tissue oxygen tension in the obstructed kidney cortex showed no change in response to AUUO (Fig. 1A). In the non-obstructed kidney, AUUO caused a small increase in tissue oxygen tension in both medulla and cortex (Fig. 1C,D). The onset of this increase was delayed approximately 10 min compared

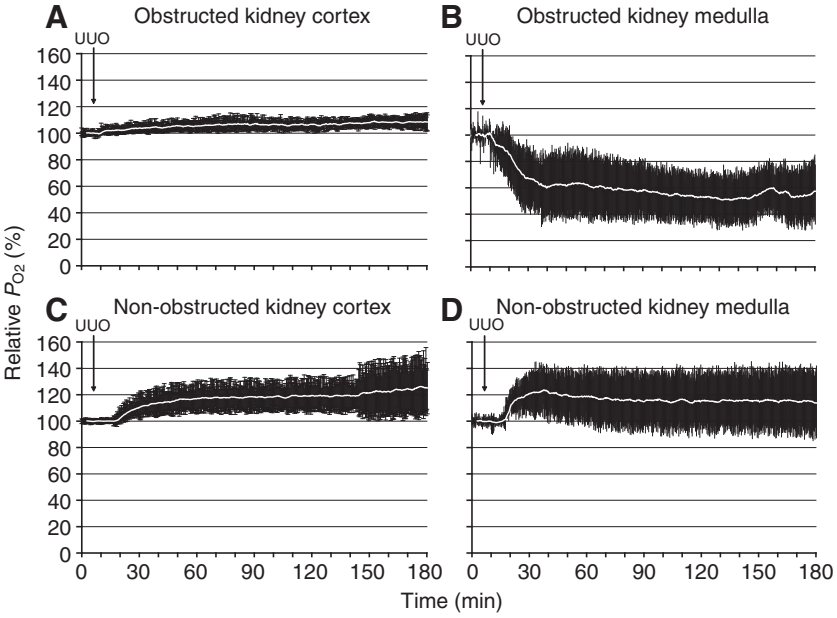

Fig. 1. Oxygen tension in obstructed and non-obstructed kidney. A period of 5 min was used to normalize the mean P_{O_2} level to 100%. In the UUO group, obstruction was initiated after 10 min, and P_{O_2} was successively recorded for up to 3 hours at intervals of 15 s. Measurements of P_{O_2} relative to baseline levels were averaged for all animals (N=8), and plotted as means ± s.d. of cortex and medulla. (A,B) Cortical P_{O_2} in the obstructed kidney remained at baseline level (A), whereas medullary P_{O_2} in the obstructed kidney decreased rapidly during the first 30 min of UUO (B). (C,D) Cortical and medullary P_{O_2} in the contralateral kidney increased slightly during the first 45 min of UUO.

with the reduced medullary tissue oxygen tension observed in the obstructed kidney, although the variation in P_{O_2} was generally high. The relative P_{O_2} level remained unchanged during the 3 h study period in the sham-operated rats, and we found no difference between the sham-operated and the contralateral kidney in this group (data not shown).

Acute unilateral ureteral obstruction changes regional renal blood flow

Changes in regional renal blood flow during AUUO were determined in the obstructed and the non-obstructed kidney by MRI. In parallel, we measured the regional renal blood flow in sham-operated control animals and found no difference between the sham-operated kidney and the contralateral kidney in these control animals (data not shown). Therefore, we choose to use only the measurements from the sham-operated kidney as control data in the analysis. The renal blood flow was measured at two time points, at baseline and at 1.5–2 h after onset of UUO, and CBF and MBF are presented as percentage changes. MBF was significantly reduced to 61±9% of baseline level in the obstructed kidney compared with 100±6% of baseline level in the sham-operated control kidney (P<0.01; Fig. 2). In the non-obstructed kidney, MBF was comparable with the sham-operated control kidney level. Furthermore, CBF increased significantly to 108±2% of baseline levels in the non-obstructed kidney compared with 97±2% of baseline levels in the sham-operated control kidney (P<0.01; Fig. 2), but remained unchanged in the obstructed kidney.

Two hours of UUO increases NKCC2 abundance in the non-obstructed kidney

Active sodium chloride reabsorption *via* NKCC2 in the medullary TAL is a major determinant of medullary oxygen consumption, as inhibition of NKCC2 by loop diuretics clearly increases medullary tissue oxygen tension (Brezis et al., 1994a). The abundance of NKCC2 in the ISOM (representing medullary TAL) of the obstructed kidney was comparable to that of the sham-operated controls. However, in the non-obstructed kidney NKCC2 abundance increased significantly to 123% of the levels in the sham-operated kidney (P<0.05; Fig. 3).

Na^+/K^+-ATPase abundance is increased in obstructed kidney inner medulla

Na^+/K^+-ATPase, is localized in the basolateral membrane of the renal tubular cells and plays a fundamental role in active sodium transport across the renal tubular epithelium (Baskin and Stahl, 1982; Katz, 1982). Na^+/K^+-ATPase protein abundance was significantly increased to 119% of the sham-operated kidney levels in the obstructed kidney IM (P<0.05; Fig. 4) but remained comparable with the sham-operated kidney levels in the non-obstructed kidney IM. In ISOM and cortex, 2 h of UUO caused no significant change in Na^+/K^+-ATPase abundance in either the obstructed kidney or the non-obstructed kidney compared with the levels in the sham-operated kidney (Fig. 4).

Two hours of UUO enhances cortical, total AQP2 abundance

Non-phosphorylated AQP2 localized in subapical vesicles in the collecting duct principal cells is oxygen-independent and so not expected to be influenced by hypoxia (Nielsen et al., 1995).

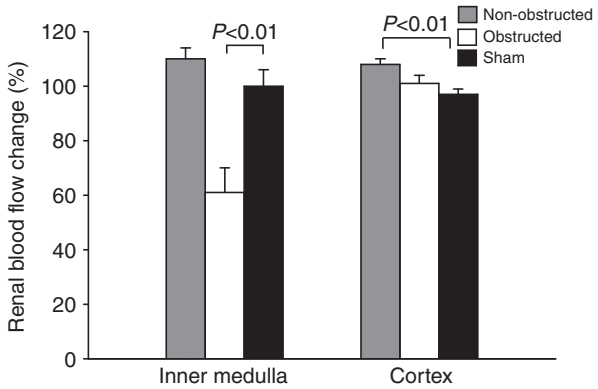

Fig. 2. Relative changes in the medullary and cortical blood flow in UUO rats (N=5) and sham-operated rats (N=7) determined by MRI; measures acquired before UUO are regarded as baseline values. The MBF was significantly reduced in the obstructed kidney from UUO rats compared with the sham-operated kidney (P<0.01). The CBF in the non-obstructed kidney was significantly enhanced compared with the sham-operated control kidney (P<0.05). Each bar represents mean ± s.e.m.

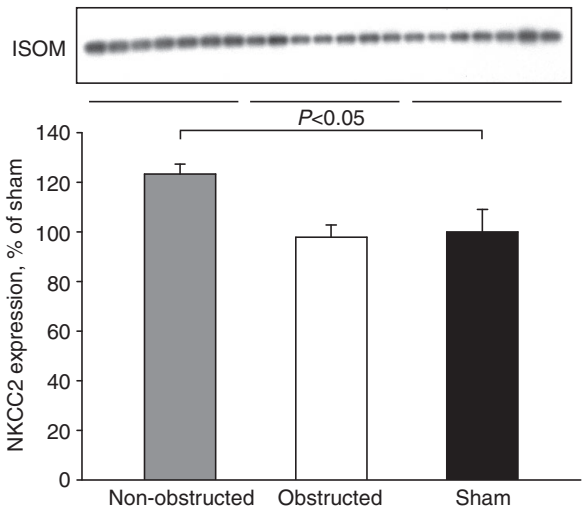

Fig. 3. NKCC2 abundance in inner stripe of outer medulla (ISOM) from rats subjected to 2 h UUO (non-obstructed right kidney, obstructed left kidney; *N*=7) and sham-operated rats (sham, *N*=7). NKCC2 abundance significantly increased in the non-obstructed kidney compared with the sham-operated kidney ($P<0.05$), whereas NKCC2 abundance in the obstructed kidney remained unchanged. Each bar represents the mean ± s.e.m.

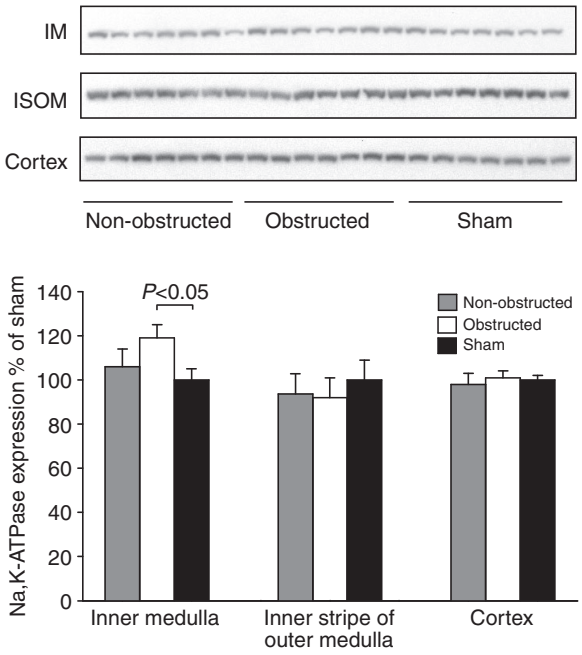

Fig. 4. Na^+/K^+-ATPase abundance in inner medulla (IM), inner stripe of outer medulla (ISOM), and cortex from rats subjected to 2 h UUO (non-obstructed right kidney, obstructed left kidney; *N*=7) and sham-operated rats (sham, *N*=7). Na^+/K^+-ATPase abundance increased significantly in obstructed kidney IM compared with the sham-operated kidney. No significant changes in Na^+/K^+-ATPase protein level were found in ISOM or cortex UUO. Each bar represents mean ± s.e.m.

However, the AQP2 antibody labels total AQP2 abundance including phosphorylated AQP2 (pAQP2), and therefore changes in pAQP2 are potentially reflected in the total AQP2 abundance. This study showed no change in medullary, total AQP2 abundance in the obstructed and the non-obstructed kidney compared with the sham-operated kidney levels. In both the obstructed and the non-obstructed kidney, the cortical, total AQP2 abundance increased significantly to 120±5% and 146±12% of sham-operated kidney levels, respectively ($P<0.05$; Fig. 5).

Cortical and medullary pAQP2 in the obstructed kidney is differently regulated in AUUO

Water transport across the apical plasma membrane of the collecting duct principal cells is facilitated by pAQP2 (Katsura et al., 1997). The water transport uses no oxygen but phosphorylation of AQP2 is oxygen-consuming and thus medullary hypoxia may influence pAQP2 abundance. Two hours of UUO caused a significant reduction in obstructed kidney inner medullary pAQP2 abundance to 66±3% of the sham-operated kidney levels ($P<0.001$; Fig. 6). By contrast, cortical pAQP2 abundance slightly increased in the obstructed kidney to 117±2% of the sham-operated kidney levels in response to 2 h UUO ($P<0.05$; Fig. 6). No significant differences were observed in the inner medullary or cortical pAQP abundance in the non-obstructed kidney compared with the sham-operated kidney.

DISCUSSION

We investigated whether cortical and medullary tissue P_{O_2}s reflect regional renal blood flow in AUUO and thus if blood flow measurements can be used as a predictor of hypoxia. Medullary tissue P_{O_2} in the obstructed kidney decreased during the first 30 min of UUO whereas cortical tissue P_{O_2} increased in the non-obstructed kidney. In agreement with these findings, there was a reduction in MBF in the obstructed kidney and a concurrent increase in the non-obstructed kidney CBF. Finally, our study showed that renal transport protein abundance changed independently of tissue P_{O_2} in specific kidney zones.

Acute unilateral ureteral obstruction influences renal regional blood flow

Renal regional blood flow in ureteral obstruction has been intensively investigated using a wide range of methods, and it is generally accepted that medullary blood flow rapidly declines in response to elevated renal pelvic pressure (Heyman et al., 1997; Schwartz et al., 1977; Solez et al., 1976; Sweeney et al., 2001; Wahlberg et al., 1984). Consistently, non-invasive MRI measurements of renal regional blood flow in rats subjected to 1.5–2 h UUO showed a marked reduction in MBF to 60% of baseline level. As MBF relies on the descending vasa recta, a low pressure vascular system, MBF is susceptible to the enhanced intrapelvic pressure in AUUO which may compress the vessels and thus reduce blood flow. Less is known about regional blood flow distribution in the non-obstructed kidney. Wahlberg et al. (Wahlberg et al., 1984) showed a tendency towards an increased blood flow in all kidney zones in response to 2 h UUO, whereas other studies have described the regional blood flow as comparable to a control group (Heyman et al., 1997; Solez et al., 1976). The present study demonstrated a significantly enhanced CBF in the non-obstructed kidney using non-invasive MRI. Contrast-enhanced dynamic MRI allows non-invasive measurements of the renal handling of water, including determination of CBF and MBF. However, these calculations are based on the assumption that cortex and medulla exhibit two-compartmental behaviour, and that the relationship between MRI signal and concentration is known. Our findings should therefore be used on a relative basis and not in absolute units.

Renal regional blood flow measurements reflects regional tissue oxygenation in AUUO

Blood flow is occasionally used as a determinant of the tissue P_{O_2} and a markedly reduced blood flow is considered as an indicator of

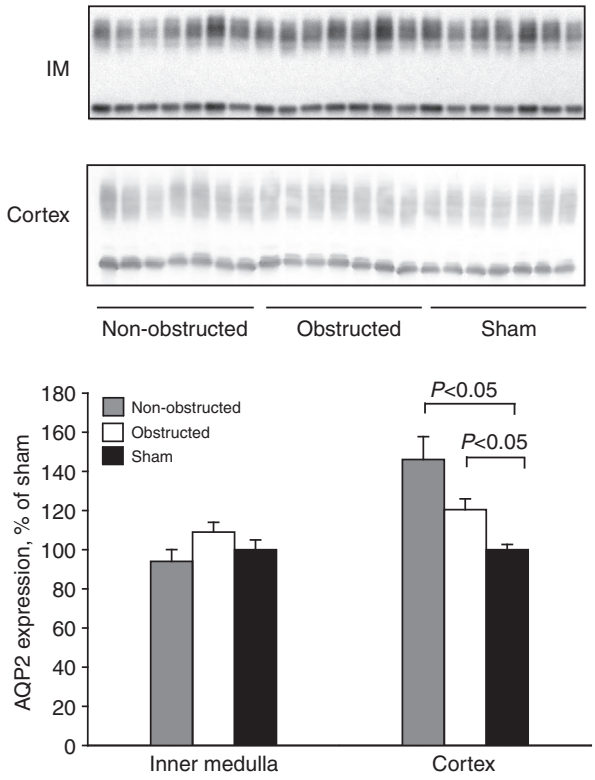

Fig. 5. Total AQP2 abundance in inner medulla (IM) and cortex from rats subjected to 2 h UUO (non-obstructed right kidney, obstructed left kidney; *N*=7) and sham-operated rats (sham, *N*=7). UUO for 2 h resulted in a significantly enhanced levels of cortical AQP2 protein in both the obstructed and non-obstructed kidney compared with that in the sham-operated kidney ($P<0.05$). AQP2 abundance in non-obstructed and obstructed kidney IM was comparable to that sham-operated kidney. Each bar represents mean ± s.e.m.

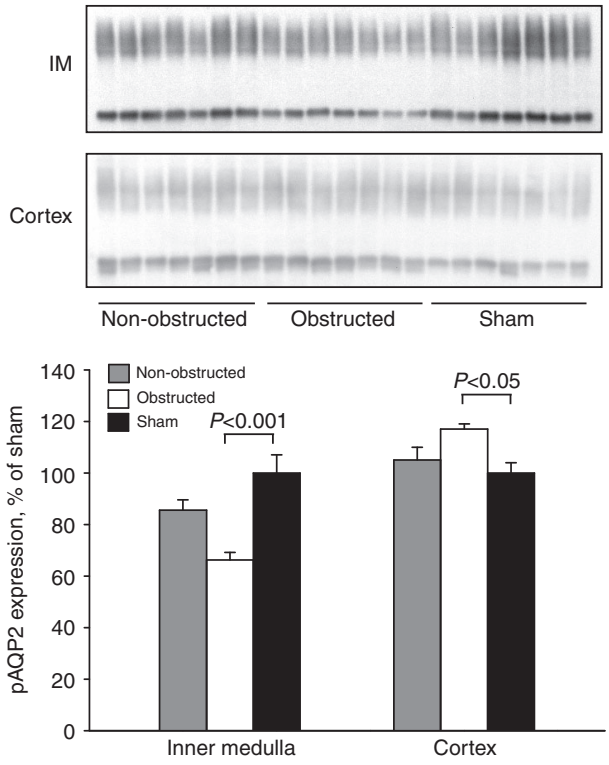

Fig. 6. Phosphorylated AQP2 (pAQP2) abundance in kidney inner medulla (IM) and cortex from rats subjected to 2 h UUO (non-obstructed right kidney, obstructed left kidney; *N*=7) and sham-operated kidney (sham, *N*=7). pAQP2 protein level decreased significantly in obstructed kidney IM ($P<0.01$), but increased in the obstructed kidney cortex compared with the level in the sham-operated kidney ($P<0.05$). No changes in pAQP2 abundance were observed in the non-obstructed kidney. Each bar represents mean ± s.e.m.

hypoxic injury although tissue P_{O_2} also depends on oxygen consumption in the specific tissue of interest. As regional renal blood flow and oxygen consumption are highly complex this assumption may not be correct in AUUO. To preserve the medullary osmotic gradients and to enhance urinary concentration the renal MBF and tissue P_{O_2} are relatively low, and even small reductions in MBF may cause hypoxic injury (for a review, see Brezis and Rosen, 1995). Our study demonstrated a clear association between regional blood flow distribution and tissue P_{O_2} during the first hours of UUO as both the MBF and tissue P_{O_2} were clearly reduced in the obstructed kidney, whereas CBF and tissue P_{O_2} increased in the non-obstructed kidney. The kidney has developed a number of defensive strategies to prevent hypoxic injury, involving vasodilatation of the descending vasa recta mediated by prostaglandins and the nitric oxide (NO) system which by increasing MBF reduces the osmotic gradients and thus decreases oxygen consumption by active solute transport (Agmon and Brezis, 1993; Agmon et al., 1994; Brezis et al., 1991; Chou et al., 1990). Furthermore, prostaglandins have a direct inhibitory effect on active transport in medullary TAL (Lear et al., 1990). These regulatory mechanisms are consistent with the previously mentioned studies showing an exacerbated MBF decline during AUUO when inhibiting the prostaglandin and the NO system (Heyman et al., 1997). The present study showed that this defence strategy was insufficient in preventing a decreased P_{O_2}, at least during AUUO, using novel micro-optodes, which have the advantage of accurately measuring the intrarenal oxygenation without consuming oxygen itself.

Renal transport protein abundance is regulated independently of regional oxygen supply

The major renal oxygen consumption is devoted to active solute transport along the nephron, in particular the establishment of the cortico-medullary concentration gradient by secondary active sodium reabsorption *via* NKCC2 in TAL driven by the Na^+/K^+-ATPase (Brezis et al., 1994a). Furosemide treatment, which blocks NKCC2, results in higher tissue oxygenation in the rat renal medulla (Brezis et al., 1994a) indicating an association between NKCC2 activity and oxygen consumption. Therefore, it may be speculated that inhibition of active solute transport would tend to reduce the need for oxygen during pathological conditions with a limited oxygen supply, and a possible mechanism for direct inhibition of active transport could be a decreased abundance of major transport proteins. However, the present study showed no clear association between the abundance of sodium transport proteins and tissue P_{O_2}, as NKCC2 was unchanged and Na^+/K^+-ATPase was actually significantly increased in the hypoxic, obstructed kidney medulla. As the present study determined the protein abundance and not the activity of the transport proteins we cannot exclude the possibility that changes in transport protein activity may play a role in the obstructed kidney medulla (Molitoris et al., 1991; Molitoris et al., 1992).

Water diffuses passively across the tubular epithelium *via* the aquaporins and although the water transport itself consumes no oxygen, phosphorylation of AQP2 is an oxygen-consuming process

which is necessary for placement of the protein in the apical membrane of the collecting duct principal cells (for a review, see Nielsen et al., 2002). Total AQP2 abundance was unchanged in obstructed kidney medulla but interestingly, oxygen-dependent phosphorylation of AQP2 decreased significantly in the hypoxic, obstructed kidney medulla, suggesting that phosphorylation is susceptible to hypoxia. However, AQP2 phosphorylation is influenced by a number of hormones including prostaglandins and angiotensin II known to be regulated in ureteral obstruction (Frokiaer et al., 1992; Frokiaer and Sorensen, 1995; Norregaard et al., 2005; Pimentel et al., 1995). This complex regulation of AQP2 phosphorylation is further emphasized by the enhanced abundance of both total AQP2 and pAQP2 in obstructed kidney cortex which may be a compensatory mechanism to ensure high collecting duct water permeability.

Surprisingly, AQP2 and NKCC2 abundance were increased in the contralateral, non-obstructed kidney compared with sham-operated control kidneys, an upregulation not observed after 24 h UUO (Li et al., 2003a; Li et al., 2003b). The mechanism behind these changes needs to be further elucidated but it might be speculated that the modestly increased CBF in the non-obstructed kidney could play a role in the AQP2 and NKCC2 upregulation. However, previous studies investigating CBF in the contralateral kidney have revealed either unchanged (Heyman et al., 1997) or only slightly and non-significantly increased CBF during AUUO (Wahlberg et al., 1984). These studies used quite different methods (laser-Doppler and microsphere technique) to measure the CBF, which may explain the discrepancy with our study. Other factors such as angiotensin II and the prostaglandins may be involved in AQP2 and NKCC2 upregulation as these two signalling mechanisms regulate AQP2 and NKCC2 in the normal kidney (Kwon et al., 2003; Kwon et al., 2005) and have been shown to influence the renal haemodynamic during AUUO (Frokiaer et al., 1996; Frokiaer et al., 1993).

In conclusion, we demonstrate that renal tissue P_{O_2} measurements are highly correlated with regional blood flow distribution in response to AUUO in both the obstructed and the non-obstructed kidney. MBF and tissue P_{O_2} decreased significantly in the obstructed kidney whereas CBF and tissue P_{O_2} increased in the non-obstructed kidney. Therefore, this study indicates that regional blood flow measurements can be used as predictors of local hypoxia during ureteral obstruction and potentially also in other conditions associated with renal ischemia. Finally, the abundance of major transport proteins changed independently of the regional changes in tissue P_{O_2} during AUUO and only phosphorylation of AQP2 seem to be susceptible to hypoxia.

LIST OF ABBREVIATIONS

AQP2	aquaporin 2
AUUO	acute unilateral ureter obstruction
CBF	cortical blood flow
GFR	glomerular filtration rate
IM	inner medulla
ISOM	inner stripe of outer medulla
MBF	medullary blood flow
MRI	magnetic resonance imaging
NKCC2	$Na^+/K^+/2Cl^-$ co-transporter
NO	nitric oxide
pAQP2	phosphorylated aquaporin 2
P_{O_2}	oxygen tension
RBF	renal blood flow
TAL	thick ascending limb
t_E	time of echo
t_R	time of recovery
UUO	unilateral ureteral obstruction

The authors wish to thank Gitte Skou for technical assistance and Yimin Shi for surgical expertise in protocol 2. The contrast agent Sinarem was a kind gift from Guerbet, Paris, France. The Water and Salt Research Centre at the University of Aarhus was established by and is supported by the Danish National Research Foundation (Danmarks Grundforskningsfond). Support for this study was provided by The Danish Medical Research Council, The University of Aarhus Research Foundation, The A.P. Møller Foundation for the Advancement of Medical Science, Aase and Ejnar Danielsen Fund, and University of Aarhus.

REFERENCES

Agmon, Y. and Brezis, M. (1993). Effects of nonsteroidal anti-inflammatory drugs upon intrarenal blood flow: selective medullary hypoperfusion. *Exp. Nephrol.* **1**, 357-363.

Agmon, Y., Peleg, H., Greenfeld, Z., Rosen, S. and Brezis, M. (1994). Nitric oxide and prostanoids protect the renal outer medulla from radiocontrast toxicity in the rat. *J. Clin. Invest.* **94**, 1069-1075.

Aumann, S., Schoenberg, S. O., Just, A., Briley-Saebo, K., Bjornerud, A., Bock, M. and Brix, G. (2003). Quantification of renal perfusion using an intravascular contrast agent (part 1): results in a canine model. *Magn. Reson. Med.* **49**, 276-287.

Baskin, D. G. and Stahl, W. L. (1982). Immunocytochemical localization of Na^+, K^+-ATPase in the rat kidney. *Histochemistry* **73**, 535-548.

Brezis, M. and Rosen, S. (1995). Hypoxia of the renal medulla-its implications for disease. *N. Engl. J. Med.* **332**, 647-655.

Brezis, M., Heyman, S. N., Dinour, D., Epstein, F. J. and Rosen, S. (1991). Role of nitric oxide in renal medullary oxygenation: studies in isolated and intact rat kidneys. *J. Clin. Invest.* **88**, 390-395.

Brezis, M., Agmon, Y. and Epstein, F. H. (1994a). Determinants of intrarenal oxygenation. I. Effects of diuretics. *Am. J. Physiol.* **267**, F1059-F1062.

Brezis, M., Heyman, S. N. and Epstein, F. H. (1994b). Determinants of intrarenal oxygenation. II. Hemodynamic effects. *Am. J. Physiol.* **267**, F1063-F1068.

Chen, C. F., Yeh, S. U., Chien, C. T. and Wu, M. S. (2001). Renal response during acute unilateral ureteral obstruction in rats. *Neurourol. Urodyn.* **20**, 125-137.

Chou, S. Y., Porush, J. G. and Faubert, P. F. (1990). Renal medullary circulation: hormonal control. *Kidney Int.* **37**, 1-13.

Christensen, B. M., Zelenina, M., Aperia, A. and Nielsen, S. (2000). Localization and regulation of PKA-phosphorylated AQP2 in response to V2-receptor agonist/antagonist treatment. *Am. J. Physiol. Renal Physiol.* **278**, F29-F42.

Dal, C. A., Stanziale, R., Corradi, A., Andreucci, V. E. and Migone, L. (1977). Effects of acute ureteral obstruction on glomerular hemodynamics in rat kidney. *Kidney Int.* **12**, 403-411.

Ecelbarger, C. A., Terris, J., Hoyer, J. R., Nielsen, S., Wade, J. B. and Knepper, M. A. (1996). Localization and regulation of the rat renal Na^+-K^+-2Cl- cotransporter, BSC-1. *Am. J. Physiol.* **271**, F619-F628.

Frokiaer, J. and Sorensen, S. S. (1995). Eicosanoid excretion from the contralateral kidney in pigs with complete unilateral ureteral obstruction. *J. Urol.* **154**, 1205-1209.

Frokiaer, J., Knudsen, L., Nielsen, A. S., Pedersen, E. B. and Djurhuss, J. C. (1992). Enhanced intrarenal angiotensin II generation in response to obstruction of the pig ureter. *Am. J. Physiol.* **263**, F527-F533.

Frokiaer, J., Nielsen, A. S., Knudsen, L., Djurhuus, J. C. and Pedersen, E. B. (1993). The effect of indomethacin infusion on renal hemodynamics and on the renin-angiotensin system during unilateral ureteral obstruction of the pig. *J. Urol.* **150**, 1557-1563.

Frokiaer, J., Djurhuus, J. C., Nielsen, M. and Pedersen, E. B. (1996). Renal hemodynamic response to ureteral obstruction during converting enzyme inhibition. *Urol. Res.* **24**, 217-227.

Gansert, D., Burgdorf, M. and Lösch, R. (2001). A novel approach to the in situ measurement of oxygen concentrations in the sapwood of woody plants. *Plant Cell Environ.* **24**, 1007-1118.

Harris, R. H. and Yarger, W. E. (1974). Renal function after release of unilateral ureteral obstruction in rats. *Am. J. Physiol.* **227**, 806-815.

Heyman, S. N., Fuchs, S., Jaffe, R., Shina, A., Ellezian, L., Brezis, M. and Rosen, S. (1997). Renal microcirculation and tissue damage during acute ureteral obstruction in the rat: effect of saline infusion, indomethacin and radiocontrast. *Kidney Int.* **51**, 653-663.

Kashgarian, M., Biemesderfer, D., Caplan, M. and Forbush, B., 3rd (1985). Monoclonal antibody to Na,K-ATPase: immunocytochemical localization along nephron segments. *Kidney Int.* **28**, 899-913.

Katsura, T., Gustafson, C. E., Ausiello, D. A. and Brown, D. (1997). Protein kinase A phosphorylation is involved in regulated exocytosis of aquaporin-2 in transfected LLC-PK1 cells. *Am. J. Physiol.* **272**, F817-F822.

Katz, A. I. (1982). Renal Na-K-ATPase: its role in tubular sodium and potassium transport. *Am. J. Physiol.* **242**, F207-F219.

Kiroytcheva, M., Cheval, L., Carranza, M. L., Martin, P. Y., Favre, H., Doucet, A. and Feraille, E. (1999). Effect of cAMP on the activity and the phosphorylation of Na^+,K^+-ATPase in rat thick ascending limb of Henle. *Kidney Int.* **55**, 1819-1831.

Kwon, T. H., Nielsen, J., Kim, Y. H., Knepper, M. A., Frokiaer, J. and Nielsen, S. (2003). Regulation of sodium transporters in the thick ascending limb of rat kidney: response to angiotensin II. *Am. J. Physiol. Renal Physiol.* **285**, F152-F165.

Kwon, T. H., Nielsen, J., Knepper, M. A., Frokiaer, J. and Nielsen, S. (2005). Angiotensin II AT1 receptor blockade decreases vasopressin-induced water reabsorption and AQP2 levels in NaCl-restricted rats. *Am. J. Physiol. Renal Physiol.* **288**, F673-F684.

Lear, S., Silva, P., Kelley, V. E. and Epstein, F. H. (1990). Prostaglandin E2 inhibits oxygen consumption in rabbit medullary thick ascending limb. *Am. J. Physiol.* **258**, F1372-F1378.

Li, C., Wang, W., Knepper, M. A., Nielsen, S. and Frokiaer, J. (2003a). Downregulation of renal aquaporins in response to unilateral ureteral obstruction. *Am. J. Physiol. Renal Physiol.* **284**, F1066-F1079.

Li, C., Wang, W., Kwon, T. H., Knepper, M. A., Nielsen, S. and Frokiaer, J. (2003b). Altered expression of major renal Na transporters in rats with unilateral ureteral obstruction. *Am. J. Physiol. Renal Physiol.* **284**, F155-F166.

Molitoris, B. A., Geerdes, A. and McIntosh, J. R. (1991). Dissociation and redistribution of Na^+,K^+-ATPase from its surface membrane actin cytoskeletal complex during cellular ATP depletion. *J. Clin. Invest.* **88**, 462-469.

Molitoris, B. A., Dahl, R. and Geerdes, A. (1992). Cytoskeleton disruption and apical redistribution of proximal tubule Na^+-K^+-ATPase during ischemia. *Am. J. Physiol.* **263**, F488-F495.

Moody, T. E., Vaughn, E. D., Jr and Gillenwater, J. Y. (1975). Relationship between renal blood flow and ureteral pressure during 18 h of total unilateral uretheral occlusion. Implications for changing sites of increased renal resistance. *Invest. Urol.* **13**, 246-251.

Neuhofer, W. and Beck, F. X. (2006). Survival in hostile environments: strategies of renal medullary cells. *Physiology (Bethesda)* **21**, 171-180.

Nielsen, J., Kwon, T. H., Praetorius, J., Frokiaer, J., Knepper, M. A. and Nielsen, S. (2006). Aldosterone increases urine production and decreases apical AQP2 expression in rats with diabetes insipidus. *Am. J. Physiol. Renal Physiol.* **290**, F438-F449.

Nielsen, S., Chou, C. L., Marples, D., Christensen, E. I., Kishore, B. K. and Knepper, M. A. (1995). Vasopressin increases water permeability of kidney collecting duct by inducing translocation of aquaporin-CD water channels to plasma membrane. *Proc. Natl. Acad. Sci. USA* **92**, 1013-1017.

Nielsen, S., Frokiaer, J., Marples, D., Kwon, T. H., Agre, P. and Knepper, M. A. (2002). Aquaporins in the kidney: from molecules to medicine. *Physiol. Rev.* **82**, 205-244.

Norregaard, R., Jensen, B. L., Li, C., Wang, W., Knepper, M. A., Nielsen, S. and Frokiaer, J. (2005). COX-2 inhibition prevents downregulation of key renal water and sodium transport proteins in response to bilateral ureteral obstruction. *Am. J. Physiol. Renal Physiol.* **289**, F322-F333.

O'Connor, P. M., Kett, M. M., Anderson, W. P. and Evans, R. G. (2006). Renal medullary tissue oxygenation is dependent on both cortical and medullary blood flow. *Am. J. Physiol. Renal Physiol.* **290**, F688-F694.

Pimentel, J. L., Jr, Montero, A., Wang, S., Yosipiv, I., el-Dahr, S. and Marinez-Maldonado, M. (1995). Sequential changes in renal expression of renin-angiotensin system genes in acute unilateral ureteral obstruction. *Kidney Int.* **48**, 1247-1253.

Schwartz, M. M., Venkatachalam, M. A. and Cotran, R. S. (1977). Reversible inner medullary vascular obstruction in acute experimental hydronephrosis. *Am. J. Pathol.* **86**, 425-436.

Solez, K., Ponchak, S., Buono, R. A., Vernon, N., Finer, P. M., Miller, M. and Heptinstall, R. H. (1976). Inner medullary plasma flow in the kidney with ureteral obstruction. *Am. J. Physiol.* **231**, 1315-1321.

Sweeney, P., Young, L. S. and Fitzpatrick, J. M. (2001). An autoradiographic study of regional blood flow distribution in the rat kidney during ureteric obstruction: the role of vasoactive compounds. *BJU Int.* **88**, 268-272.

Van Why, S. K., Mann, A. S., Ardito, T., Siegel, N. J. and Kashgarian, M. (1994). Expression and molecular regulation of Na^+-K^+-ATPase after renal ischemia. *Am. J. Physiol.* **267**, F75-F85.

Von Willert, D., Matyssek, R. and Herppich, W. (1995). *Experimentelle Pflanzenökologie: Grundlagen und Anwendungen*. Stuttgart: Georg Thieme Verlag.

Wahlberg, J., Karlberg, L. and Persson, A. E. (1984). Total and regional renal blood flow during complete unilateral ureteral obstruction. *Acta Physiol. Scand.* **121**, 111-118.

Wang, Z., Rabb, H., Haq, M., Shull, G. E. and Soleimani, M. (1998). A possible molecular basis of natriuresis during ischemic-reperfusion injury in the kidney. *J. Am. Soc. Nephrol.* **9**, 605-613.